Final Draft
of the original manuscript:

Guo, Y.; Wang, Y.; Qi, H.; Steglich, D.:
Atomistic simulation of tension deformation behavior in magnesium single crystal
In: Acta Metallurgica Sinica (English Letters) (2010) Elsevier
2010 Vol. 23 (5): 370 - 380

DOI: -

Atomistic simulation of tension deformation behavior in magnesium single crystal

Yafang GUO 郭雅芳 [1)*], Yuesheng WANG 汪越胜 [1)], Honggang QI 亓宏刚 [1)] and Dirk STEGLICH [2,3)]

1) Institute of Engineering Mechanics, Beijing Jiaotong University, Beijing 100044, China

2) GKSS Research Centre, Institute of Materials Research, Materials Mechanics, D-21502 Geesthacht, Germany

3) G.I.F.T., Pohang University of Science and Technology, Pohang, Gyeongbuk, 790-784, Korea

Abstract

The deformation behavior in magnesium single crystal under c-axis tension is investigated in a temperature range between 250 K and 570 K by molecular dynamics simulations. At a low temperature, twinning and shear bands are found to be the main deformation mechanisms. In particular, the $\{10\bar{1}2\}$ tension twins with the reorientation angle of about 90° are observed in the simulations. The mechanisms of $\{10\bar{1}2\}$ twinning are illustrated by the simulated motion of atoms. Moreover, grain nucleation and growth are found to be accompanied with the $\{10\bar{1}2\}$ twinning. At temperatures above 450K, the twin frequency decreases with increasing temperature. The $\{10\bar{1}2\}$ extension twin almost disappears at the temperature of 570K. The non-basal slip plays an important role on the tensile deformation in magnesium single crystal at high temperatures.

KEYWORDS Atomistic simulations; Magnesium; Twinning; c-axis tension

1. Introduction

Magnesium alloys have attracted attention in recent years as lightweight materials for the transportation industry due to their low density and relatively high specific strength. However, the

* Corresponding author. Associate professor, PhD, Tel: +86-10-51682094; Fax: 86-10-51682094.
E-mail address: yfguo@bjtu.edu.cn (Yafang GUO)

application of magnesium alloys is restricted due to the limited forming capacity and the poor corrosion resistance. From the mechanical point of view, magnesium and its wrought alloys show a pronounced direction-dependence of plastic yielding and work hardening, as well as different yielding behavior in tension and compression, the so-called strength differential (SD) effect [1]. This feature is due to the crystal structure of magnesium, which is a hexagonally close-packed (hcp) structure. Compared to face-centered cubic (fcc) or body-centered cubic (bcc) metals, the number of slip systems allowing plastic deformation in magnesium is limited. As a consequence, the material deforms by twinning, which is usually regarded as the dominant deformation mode.

One possibility to address the micromechanical deformation mechanisms is the investigation of single crystals of pure magnesium, which show the same or similar principal features as magnesium alloys. Planes and orientations of the hexagonal lattice are usually described with the Miller-Bravais indices related to a coordinate system of three basal vectors, $\mathbf{a}_1, \mathbf{a}_2, \mathbf{a}_3$, and the longitudinal axis, c, which is the axis of hexagonal symmetry. Within this system, four axes are used rather than three orthogonal ones. Dislocations in a hexagonal lattice may be grouped in three families, $\langle \mathbf{a} \rangle, \langle \mathbf{c} \rangle$ and $\langle \mathbf{a}+\mathbf{c} \rangle$, depending on the orientation of the slip plane and the slip directions, with the respective Burgers vectors of lengths a, c and $\sqrt{a^2+c^2}$. The basal plane is characterized by its normal vector $\mathbf{n} = \{0001\}$, the prismatic planes by $\mathbf{n} = \{\bar{1}100\}$ and the pyramidal planes by $\mathbf{n} = \{01\bar{1}1\}$, $\mathbf{n} = \{11\bar{2}2\}$ and $\mathbf{n} = \{10\bar{1}2\}$. Straining in direction of the c-axis can only be accommodated by $\langle \mathbf{c}+\mathbf{a} \rangle$-systems, with a slip direction of $\mathbf{m} = \langle 11\bar{2}3 \rangle$ on the pyramidal plane $\mathbf{n} = \{11\bar{2}2\}$.

Beside the deformation caused by slip along crystallographic planes, deformation twinning is an important deformation mechanism for hcp metals. It might generally be of tensile or compressive nature, depending whether it results in an elongation or reduction of the c-axis length. Experimental results have revealed that there exist two main deformation twin modes for magnesium: the $\{10\bar{1}2\}\langle 10\bar{1}1 \rangle$ c-axis tension twinning [1,2], and the $\{10\bar{1}1\}\langle 10\bar{1}2 \rangle$ c-axis compression twinning [3]. The $\langle 10\bar{1}1 \rangle$-$\langle 10\bar{1}2 \rangle$ double twinning has also been observed by electron backscattering diffraction [4,5] as two subsequent reorientations of a volume under monotonously increasing load. The microstructure mechanisms of deformation in pure magnesium have been modeled by visco-plastic constitutive equations of crystal plasticity by using finite element simulations [6]. Recently, mechanisms for $\{10\bar{1}2\}$ twinning in hcp crystals were studied by atomistic simulations [7,8]. Due to the hcp structure of magnesium, the $\{10\bar{1}2\}$

twinning cannot be accomplished by a homogeneous shear. The mechanism of the $\{10\bar{1}2\}$ twinning is still under discussion [9,10].

Moreover, the deformation behavior of magnesium is found to be very sensitive to temperatures [11]. Above about 0.3Tm (Tm being the absolute melting point), a strong decrease in the work hardening with increasing temperature is observed. Simultaneously, the ductility is increasing. A connection has often been made between the increased ductility of magnesium single crystals and the increased activity of non-basal slip that is observed at elevated temperatures [11,12]. Besides, there was clear evidence of dynamic recrystallization at elevated temperatures in magnesium alloys [13]. Dynamic recrystallization is also thermally activated and known to enhance the ductility of magnesium alloys. A mechanistic explanation for the plastic behavior of a wrought magnesium alloy has been developed recently by using a combination of experimental and simulation techniques [13]. It is indicated that increased non-basal slip activity provides a satisfying explanation for the improved formability of magnesium at elevated temperatures, and that dynamic recrystallization processes are also important for improving the ductility of this hcp metal at high temperatures.

In general, the significance of deformation mechanisms acting in magnesium and its alloys and the twinning modes in particular are still subjected to discussion. One additional methodology to clarify the deformation mechanisms in magnesium besides experimental techniques on the micro- and macroscale is an atomistic-scale description which can contribute for the understanding of the deformation behavior. In the present paper, molecular dynamics simulations are applied to investigate the tensile deformation behavior in Magnesium single crystal at different temperatures. The deformation mechanisms at different temperatures are discussed.

2. Conditions of computer simulations

For the molecular dynamics simulations, a plane representation of the lattice of magnesium atoms is considered. Its orientation is included in Fig. 1a: The X axis is oriented along the $[\bar{1}010]$ direction, the Y axis along the $[0001]$ direction, and Z axis along the $[\bar{1}2\bar{1}0]$ direction. A plane strain problem is considered in the simulations to reduce computational cost compared to full 3D simulations, and a periodic boundary condition is applied in the $[\bar{1}2\bar{1}0]$ (Z) direction. In Fig. 1b, the atomic positions in a

hcp crystal (c/a-ratio is 1.623.) are shown. It can be seen that the atoms align in layers along the $[\bar{1}2\bar{1}0]$ direction periodically with the sequence of …ABAB…: Atoms in layer A are marked as hollow circles, while atoms in layer B as solid circles. Thus, the atomic arrangement can be displayed in one plane, including atoms from layer A and B, as shown in Fig. 1c. The outmost four layers of atoms in the upper and bottom sides of the model are identified as the boundary region in atomistic simulations, shown in figure 2 as black regions in the atomistic models. The thickness of the boundary region is chosen to be larger than the cut-off distance of the potential. During the whole simulations, a free boundary condition is applied in the X direction, and a fixed-displacement boundary condition is applied both in X and Y direction for the boundary region. The EAM potential for Magnesium developed by Liu et al. by fitting to both ab initio forces and experimental data [14] is used in this work, which is proved to give good results for various bulk structural properties [8,14-16]. The XMD program [17] is used for the atomistic simulations.

Initial configurations of Magnesium single crystal samples are first defined in the simulations. Then all atoms in the model are shifted from their positions in a perfect crystal to positions specified by different values of strain along the c-axis (Y direction). Subsequently, atoms are fully relaxed for 10000 steps of magnitude 6×10E-15 s with the fixed-displacement boundary condition, and the evolution of atomic positions in the crystals at different loading levels is investigated. After a study of different values of the imposed strain, it is found that twinning can be clearly observed when the value of strain is up to 0.08. This value has been used throughout this contribution. The temperature of the system is kept constant during the simulation, which is achieved by scaling the instantaneous velocities of all atoms with the appropriate Maxwell-Boltzmann distribution at a specified temperature.

Several systems of different sizes were tested beforehand. It was verified that the basic results of the structure evolution in the simulations are neither affected by the presence of the fixed boundary nor sensitive to the change of the system size once the considered atomistic region is sufficiently large. In the simulations presented here, system with dimensions of 27×48×2.2 nm containing 160000 atoms is studied.

Information about the glide and twinning is obtained by visually following the computed displacements of atoms in the material. Once in a volume of localized displacements a typical regular (reoriented) structure is visible, this is attributed to be a twin. On the other hand, if the atomic

arrangement does show a specific periodic arrangement but is not reoriented, this is attributed to be shear band. Once regions with an irregular arrangement of atoms evolve, it is neither a twinned region nor a shear band.

3. Deformation behavior of Magnesium single crystal under tension

3.1 Deformation behavior as a function of temperature

Figure 2 shows atomistic configuration of Magnesium single crystal after a positive displacement is applied along the [0001] direction (c axis extension) at 250K, 298K, 350K, 450K, 500K and 570K, respectively. At low temperatures, twinning is found to be the dominant mechanism for accommodating deformation. When the temperature is below 450 K, as shown in Fig. 2a-d, $\{10\bar{1}2\}$ many twinned regions exist in Magnesium single crystal. The reorientation angle of the $\{10\bar{1}2\}$ twin between the twinned volume and the original matrix is about 90°. It is noticed that the $\{10\bar{1}2\}$ twin frequency increases with the temperature increasing. However, at temperatures above 450K as shown in fig. 2e and f, the $\{10\bar{1}2\}$ twin frequency decreases with the temperature increasing. In Fig. 2e, it is clearly observed that the $\{10\bar{1}2\}$ twin frequency reduces at 500 K compared with that at 450 K. In Fig. 2f at 570 K, the $\{10\bar{1}2\}$ twin has almost disappeared.

Moreover, in Fig. 2 it is noticed that the perfect lattice of magnesium single crystal is segmented into different parts by strips after a tensile load is applied. When the temperature is below 450K, these strips are found to be either twin strips or shear bands. In both cases the atomic alignment in the strip is always regular. Although strips can still be observed at temperatures above 450 K, the atomic alignment in the strip-like region is irregular. Thus neither twin strips nor shear bands exist at higher temperatures. These strip-like regions are slip traces caused by the slip of the pyramidal dislocation due to the thermal activity at higher temperatures. As shown in Fig. 2, new grains with different orientations from the original crystal are found to nucleate and grow with the $\{10\bar{1}2\}$ twinning. The grain boundary is mainly along the $\{10\bar{1}2\}$ twin boundary. Experimental observations [18-19] revealed that small dynamically recrystallized grains nucleate and grow at the original twin boundaries. After new grain formation, twin will disappear while the twin boundary becomes the grain boundary. The simulated results are in good agreement with these experimental observations.

In Fig. 2 just an overall and brief description of tension deformation behaviors in Magnesium single crystal at different temperatures is given. It's noticed that the fixed-displacement boundary condition for the boundary region has an effect on the nucleation of the twin. As shown in Fig. 2a, a twin is found nucleated near the boundary region due to the fixed-displacement boundary. However, it can be observed that most of twins are nucleated at the surface. The nucleation at the boundary region has no obviously influence on the whole deformation behavior, especially the type and mechanism of twinning. In the next sections, the atomistic details of the twin, the shear band and the slip trace will be described.

3.2 Twins and shear bands at low temperatures

Figure 3 shows the atomistic configurations at different relaxation time steps for the temperature of 298 K. As shown in Fig. 3a, after 450 steps relaxation a $\{10\bar{1}2\}$ twin (T1) forms in the left edge. In the right edge, the nucleation of $\{10\bar{1}2\}$ twins (T2 and T3) can be observed. In Fig. 3b, after 1000 steps relaxation, all twins (T1), (T2) and (T3) are grown rapidly. Moreover, some strips are also observed in the elongated crystal. For example, a $(\bar{1}011)$ twin strip exists just below (T1), thus a $\{10\bar{1}1\}$-$\{10\bar{1}2\}$ double twin forms. Below (T3), a $(\bar{1}011)$ twin strip is observed. In Fig. 3c after 2000 steps relaxation, more and more strips appear. However, the atomistic structures of strips are various. Most strips are $(\bar{1}011)$ twins, while shear bands are observed in the nether right of the figure (a detailed description see the last paragraph of this section). In some regions where the twins or shear bands meet, the atoms are arranged irregularly. Besides, it is found that (T1) and (T3) are connected after 2000 steps relaxation. In Fig. 3d after a full relaxation, a new $(\bar{1}011)$ twin forms in the right of (T1). Meanwhile, the width of the crystal is found to be reduced as a consequence of the applied tensile load.

Figures 4 zooms in the indicated regions shown in Fig. 2b and c (left square). Atomistic structures of $\{10\bar{1}2\}$ twin and $(\bar{1}011)$ twin can be clearly observed in Figs. 4a and b. Open and solid circles indicate atoms in two neighboring layers named A and B, respectively. At 350 K as shown in Fig. 4a, a $(10\bar{1}2)$ twin forms along the $[\bar{1}011]$ direction with a $(10\bar{1}2)$ twin plane. The atomic arrangement is found to be symmetrical about the $(10\bar{1}2)$ twin plane. Lines are constructed to show the overall rotation in the twinned volume. The reorientation angle α between the original matrix and the $(10\bar{1}2)$ twinned region is about 86°. At the temperature of 298 K in Fig. 4b, both $(10\bar{1}2)$ twin and $\{\bar{1}011\}$ twin are observed. Left in Fig. 4b, a $(10\bar{1}2)$ twin formed with the reorientation angle α of about 86°. On the right, a

two-layered $(\bar{1}011)$ twin is formed along the $[10\bar{1}2]$ direction with a $(\bar{1}011)$ twin plane. The atomic arrangement in the twined region is symmetric to the original matrix about the $(\bar{1}011)$ twin plane. The reorientation angle β between the original matrix and the twinned volume is about 56°. It is noticed that the atoms are arranged irregularly in the upper part of Fig. 4b where the $(\bar{1}011)$ twin and $(10\bar{1}2)$ twin meet.

Besides the twin strips, shear bands are widely observed at low temperatures under the c-axis extension. Fig. 5 zooms in particular square regions indicated in Fig. 2a and c (right square). In Fig. 5a, a regular shear band is observed at 250K, which is caused by the relative displacement of $(\bar{1}011)$ atomic layers, such as layers A and B, along the $[10\bar{1}2]$ direction by shear. Atomic arrangement in the $(\bar{1}011)$ plane has no change after the shearing. However, the shear band in Fig. 5a is no longer with a hcp structure, thus this newly formed strip is not a twin. It is not symmetrical to the original matrix on the atomistic scale. In Fig. 5b, a shear band is observed. It is also formed by the movement of layers A and B along the $[10\bar{1}2]$ direction by shear. It can be concluded from Figs. 2 and 5 that shear band is also a deformation way at low temperature under a c-axis extension. This is consistent with the experimental observation that shear bands are commonly found in cold rolled magnesium alloys [24]. This shear band is caused by a shear in the $\{10\bar{1}1\}$ plane along the $\langle 10\bar{1}2\rangle$ direction.

3.3 Mechanism of $(\bar{1}012)$ twinning

Both, shear band and the $(\bar{1}011)$ twin, are formed by shear along the $(\bar{1}011)$ plane. However, the mechanism of the $(\bar{1}012)$ twinning is different. In Fig. 6 the nucleation and formation of a $\{10\bar{1}2\}$ twin (T1 at 298 K) at two different relaxation time steps are illustrated. As shown in Fig. 6a after 250 steps relaxation, a $(\bar{1}012)$ twin unit B (identified as dashed square) nucleates, which is symmetrical to unit A about the $(\bar{1}012)$ twin plane. Arrows indicate the displacements of atoms. In Fig. 6b after 450 steps relaxation, it is found that twin grows up. A multilayer twin has formed, which can be observed also in Fig. 3a as (T1). Atoms below the $(10\bar{1}2)$ twin plane are symmetrical to atoms above the $(10\bar{1}2)$ twin plane, where the twin boundary is identified as a dash dot line. Atomic displacements can be identified by the arrows.

Fig. 7 visualizes the mechanism of $(\bar{1}012)$ twinning in detail. Atoms above the twin plane have the

initial hcp structure. Below the twin plane, atomic displacements in a twinning structure with the $(\bar{1}012)$ twin plane are presented. Two typical units A and B, identified as dashed squares, are selected, which are symmetrical about the $(\bar{1}012)$ twin plane. In order to identify the atomic positions and observe the atoms motion, some typical atoms in a twinning unit B marked as 1 to 8 are selected. It can be observed in Fig. 7 that atoms 6 and 8 move along the $[\bar{1}010]$ direction on the basal plane, while atoms 7 and 9 move along the $[000\bar{1}]$ direction on the prismatic plane. Meanwhile, atom 1 moves along the $[\bar{1}011]$ direction on the $(\bar{1}012)$ twin plane, which causes the formation of stacking faults. For atoms 2, 3, 4 and 5, only small displacements can be observed. A stretch in the $[0001]$ direction and a compression in the $[\bar{1}010]$ direction are implemented by these small displacements, which finally results in a $(\bar{1}012)$ twin formation as shown in unit B. It is noticed that the displacements of atoms in Fig. 6 obtained by atomistic simulations are consistent with atomic displacements described in Fig. 7. It can be found that the $\{10\bar{1}2\}$ twinning is achieved by two processes, the formation of stacking faults for atoms in layer A, and the basal and the prismatic slip for atoms in layer B. They nucleate and slip simultaneously, resulting in a stable twin nucleus. Therefore, the $\{10\bar{1}2\}$ twinning in magnesium single crystal can not be obtained only by a shear on the $\{10\bar{1}2\}$ twin plane. It is calculated in atomistic scale that the tensile strain that the $\{10\bar{1}2\}$ twin may accommodate is 0.067.

3.4 Slip traces at high temperatures

At higher temperatures strip-like region is widely exist, as shown in Fig. 2e and f. The perfect lattice of magnesium single crystal is segmented into different parts by strips after a tensile load is applied. Fig. 8 zooms in particular square regions shown in Fig. 2e and f. It gives the details of the atomistic structure at 500 K and 570 K. At 500 K (Fig. 8a) neither twin strips nor shear bands exist. Twinning has given way to non-basal slip above 473 K as it is observed in experiments [3]. The atomic alignment in the strip-like region is irregular. These strip-like regions are slip traces caused by the slip of the pyramidal dislocation, evidently activated at higher temperatures only. For 570 K in Fig. 8b, slip traces are clearly observed. Moreover, point defects and interstices are also found to be formed in some regions, which finally cause crack formation and failure of magnesium single crystal.

4. Discussion and Conclusions

In the simulations presented here, the $\{10\bar{1}2\}$ twinning is found to be the main deformation mechanism in magnesium single crystal under the c-axis tension at low temperatures. This is consistent with several experimental observations, e. g. [1,2]. Moreover, slip systems having a deformation component in the c-direction were considered to play a role in plastic deformation at low homologous temperatures by experiments [21-23]. In our simulations, both shear bands and the $\{\bar{1}011\}$ twinning are found under the c-axis tension, which are both caused by the shear of the $\{\bar{1}011\}$ plane. This result agrees well with the experimental observation that the dominant features of the microstructure were twins and shear bands on some clod rolled magnesium alloys [20]. Furthermore, Schmid factor analysis based on experimental results indicated that the twinning favorably occurs on the twinning plane with the highest values of Schmid factor [24]. For pure magnesium under plane strain condition as conducted in the present simulations, Schmid factors for $(10\bar{1}1)$ and $(10\bar{1}2)$ slip of 0.4153 and 0.4989 are calculated, respectively. Hence, the shear stress on the $(10\bar{1}2)$ slip plane is larger than that of the $(10\bar{1}1)$ slip plane. Therefore, it is found that the $\{10\bar{1}2\}$ twinning has priority to $\{\bar{1}011\}$ twinning at low temperatures for this loading case.

The evolving twin structures and the mechanisms of $\{10\bar{1}2\}$ twinning have been described in the previous chapter. It can be found that the $\{10\bar{1}2\}$ twinning in magnesium single crystal can not be obtained only by a shear on the $\{10\bar{1}2\}$ twin plane. The $\{10\bar{1}2\}$ twinning is achieved by two processes, the formation of stacking faults for atoms in layer A, and the basal and the prismatic slips for atoms in layer B. They nucleate and slip simultaneously, resulting in a stable twin nucleus. Thermal activity at higher temperatures is favorable for the slip and the generation of stacking faults. Thus in the simulation it is found that the $\{10\bar{1}2\}$ twin frequency increases with the temperature increasing for temperatures below 450 K. Meanwhile, new grains with different orientation nucleate and grow with the $\{10\bar{1}2\}$ twin, while the $\{10\bar{1}2\}$ twin reorients the basal plane by about 86°. The authors interpret this effect as a thermally activated recrystallization, which would improve the ductility at elevated temperatures [13, 25]. However, at temperatures above 450 K, the $\{10\bar{1}2\}$ twin frequency decreases with increasing temperature due to the activity of the non-basal slip. The $\{10\bar{1}2\}$ extension twin almost disappears at the temperature of 570 K. The non-basal slip plays then an important role for the tensile deformation,

which would be mainly responsible to the increased ductility of magnesium single crystals at high temperatures.

It has to be mentioned that the applied strain in the sample is 0.08 in the present work, and a quasi-static relaxation is applied. It is also observed that the deformation behavior varies with the applied strain and the loading rate. Thus, the present investigations represent only a small part of the possible loading situations and boundary conditions. In particular, the effect of boundary conditions on the nucleation and growth of the twins should be further investigated. It can be speculated on the effect of the plane strain assumption, which holds for all results presented here.

Acknowledgements

The research was supported by Chinese Nature Science Foundation (Grant No. 10672016 and 10632020)，the Fundamental Research Funds for the Central Universities, and finalized during a sabbatical leave of D.S. at the Graduate Institute of Ferrous Technology (G.I.F.T.) of POSTECH, Pohang, Korea as part of an international outgoing fellowship (Marie Curie Actions) of the 7th programme of the European Commission. The authors acknowledge the respective support.

References

[1] C. S. Roberts, Magnesium and its alloys (John Wiley & Sons, New York, 1960).

[2] M. R. Barnett, Mater. Sci. Eng. A 464 (2007) 1.

[3] M. R. Barnett, Mater. Sci. Eng. A 464 (2007) 8.

[4] M. R. Barnett, Z Keshavarz, A. G. Beer and X. Ma, Acta Mater. 56 (2008) 5.

[5] L. Jiang, J. J. Jonas, A. A. Luo, A. K. Sachdev and S. Godet, Scripta Mater. 54 (2006) 771.

[6] S. Graff, W. Brocks and D. Steglich, Int. J. Plast. 23 (2007)1957.

[7] J. Wang, J. P. Hirth and C. N. Tomé, Acta Mater. 57 (2009) 5521.

[8] B. Li and E. Ma, Phys. Rev. Lett. 103 **(**2009) 035503.

[9] A. Serra, D. J. Bacon and P. C. Pond, Phys. Rev. Lett. 104 **(**2010) 029603.

[10] B. Li and E. Ma, Phys. Rev. Lett. 104 (2010) 029604.

[11] K. Máthis, K. Nyilas, A. Axt, I. Dragomir-Cernatescua, T. Ungár and P. Lukáč, Acta Mater. 52 (2004) 2889.

[12] S. R. Agnew and Ö. Duygulu, Int. J. Plast. 21 (2005) 1161.

[13] A.Galiyev, R. Kaibyshev and G. Gottstein, Acta Mater. 49 (2001) 1199.

[14] X. Y. Liu, J. B. Adams, F. Ercolessi and J. A. Moriarty, Modelling Simul. Mater. Sci. Eng. 4 (1996) 293.

[15] D. L. Olmsted, L. G. Hector Jr. and W. A. Curtin, J. Mech. Phys. Solids. 54 (2006) 1763.

[16] X. Y. Liu and J. B. Adams, Acta Mater. 46 (1998) 3467.

[17] J. Rifkin, XMD - Molecular Dymamics for Metals and Ceramics. Available from: http://xmd.sourceforge.net/.

[18] D. L. Yin, K. F. Zhang, G. F. Wang and W. B. Han, Mater. Sci. Eng. A 392 (2005) 320.

[19] M. M. Myshlyaev, H. J. McQueen, A. Mwembela and E. Konopleva, Mater. Sci. Eng. A 337 (2002) 121.

[20] M. R. Barnett, M. D. Nave and C. J. Bettles, Mater. Sci. Eng. A 386 (2004) 205.

[21] J. F. Stohr and J. P. Poirier, Philos. Mag. 25 (1972) 1313.

[22] T. Obara, H. Yoshinga and S. Morozumi, Acta Metall. 21 (1973) 845.

[23] S. Ando and H. Tonda, Mater. Trans. JIM 41 (2000) 1188.

[24] L. Jiang, J.J. Jonas, R. K. Mishras, A.A. Luo, A. K. Sachdev and S. Godet, Acta Mater. 55 (2007) 3899.

[25] L. Wu, A. Jain, D. W. Brown, G. M. Stoica, S.R. Agnew, B. Clausen, D. E. Fielden and P. K. Lian, Acta Mater. 56 (2008) 688.

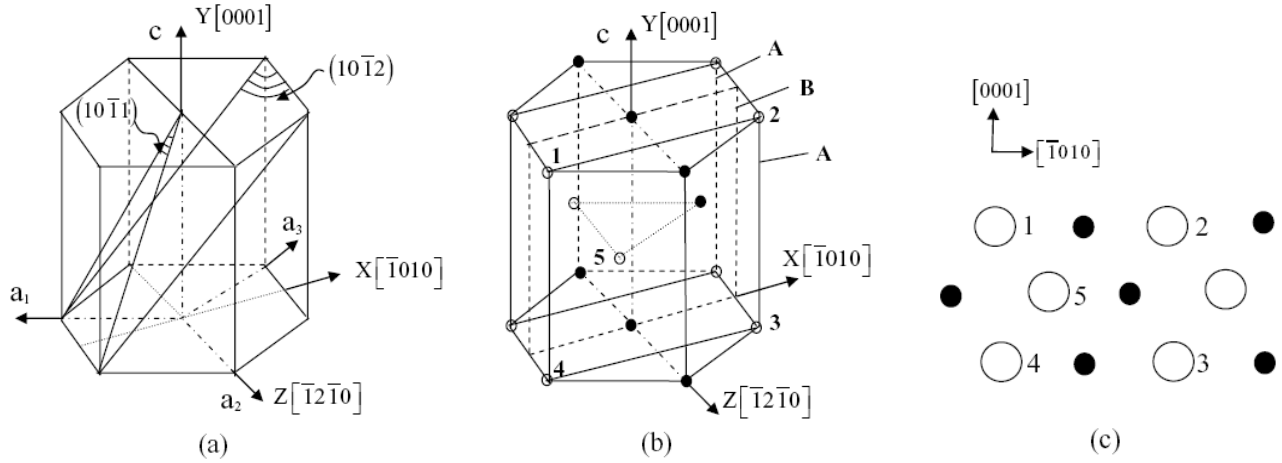

Fig.1 Lattice structure of the hcp crystal (a), periodic arrangement of atoms (b) and its plane representation (c).

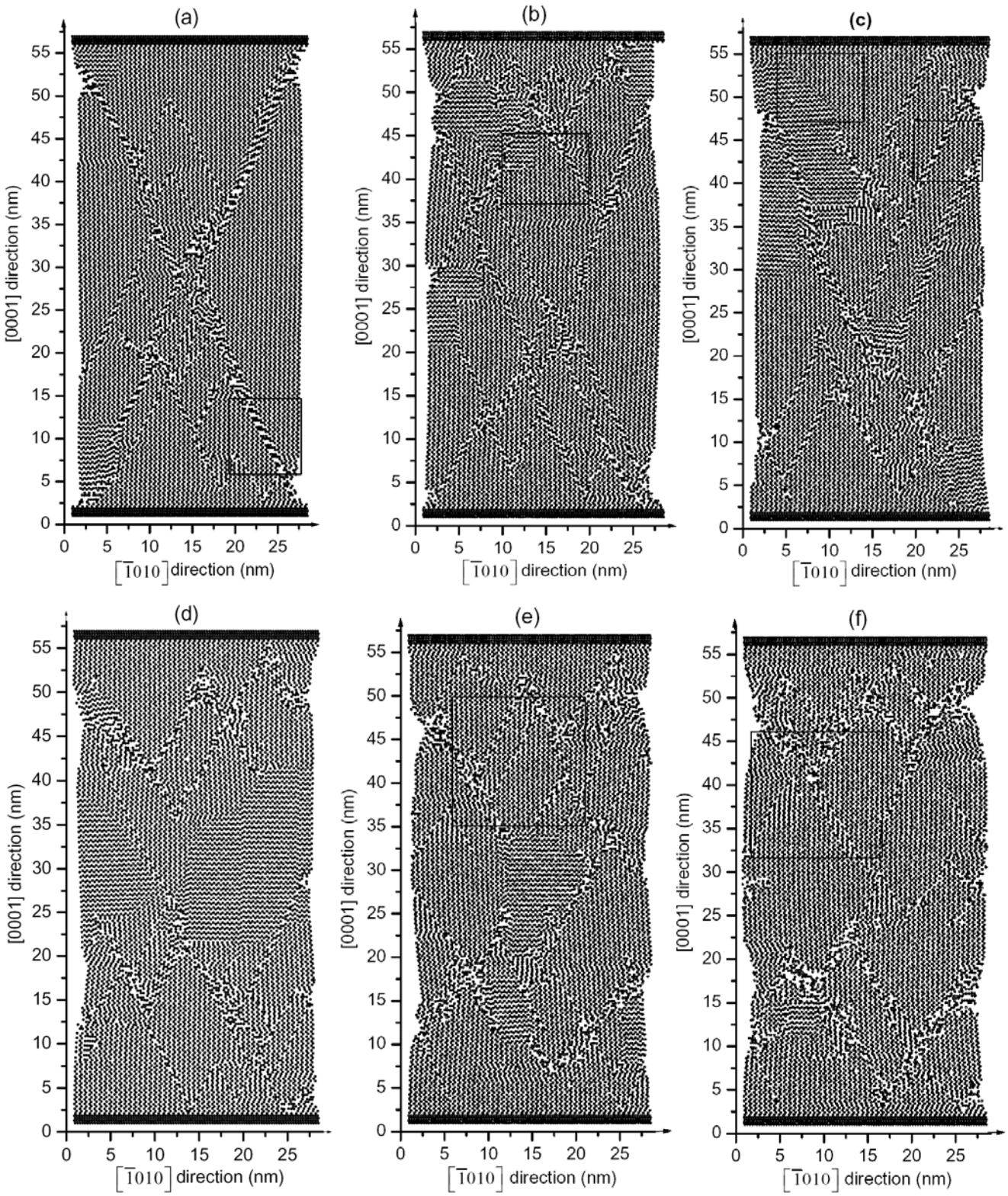

Fig.2. Atomistic configuration of Magnesium single crystal under a c-axis extension at: (a) 250K; (b) 298 K; (c) 350K; (d) 450K; (e) 500K; and (f) 570K. Above 450K, the twin frequency decreases with the temperature increasing. The $\{10\bar{1}2\}$ extension twin with the reorientation angle of about 90° almost disappears at the temperature of 570K. The squares refer to details presented in Figs. 4, 5 and 8.

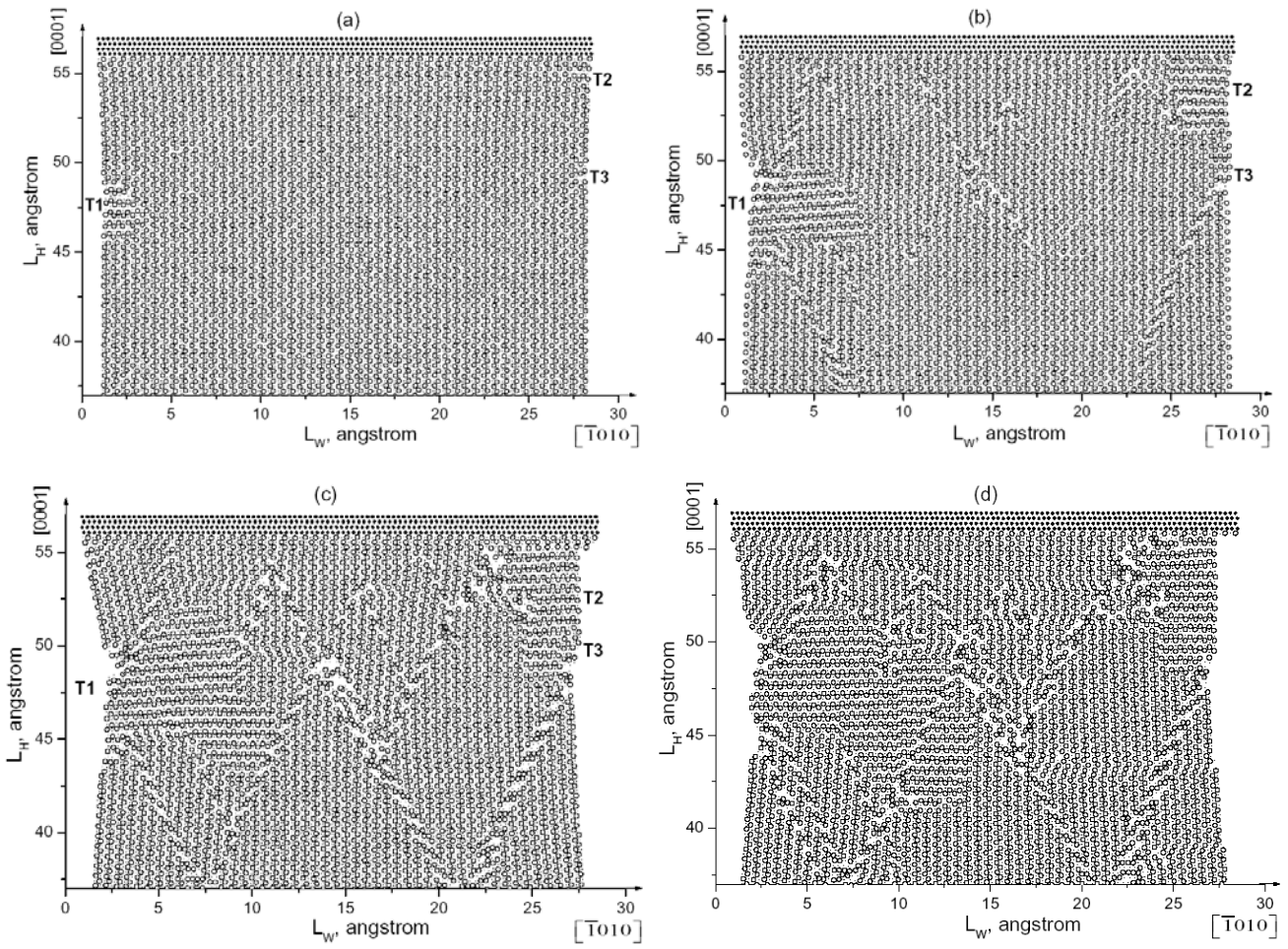

Fig. 3. Atomistic configuration of Magnesium single crystal under a c-axis tension at 298K after: (a) 450 steps relaxation; (b) 1000 steps relaxation; (c) 2000 steps relaxation; (d) 10000 steps relaxation.

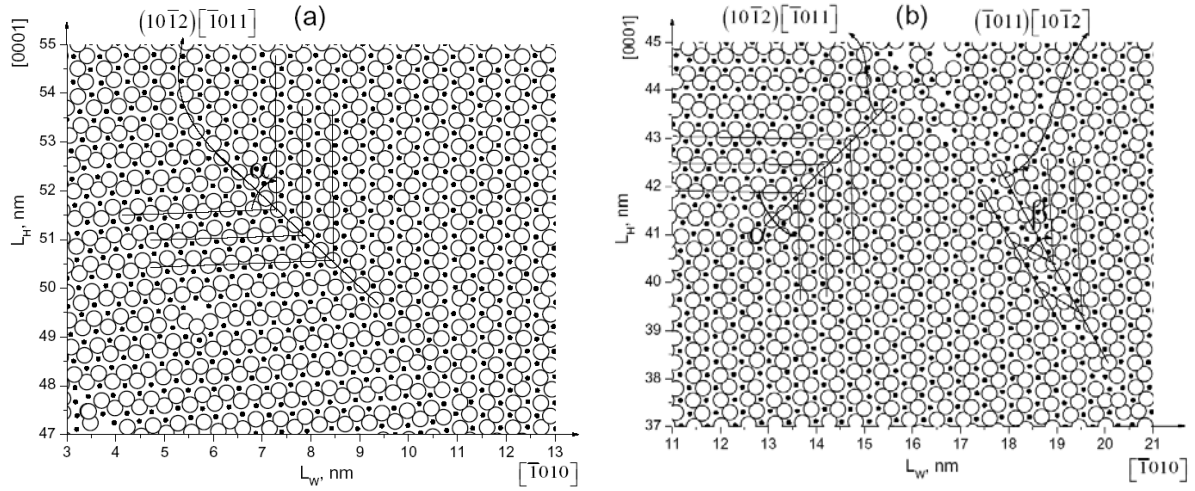

Fig.4. Atomistic structure of: (a) a $\{10\bar{1}2\}$ twin at 350 K; and (b) a $\{10\bar{1}1\}$ and a $\{10\bar{1}2\}$ twin at 298 K. Open and solid circles indicate atoms in A and B layers.

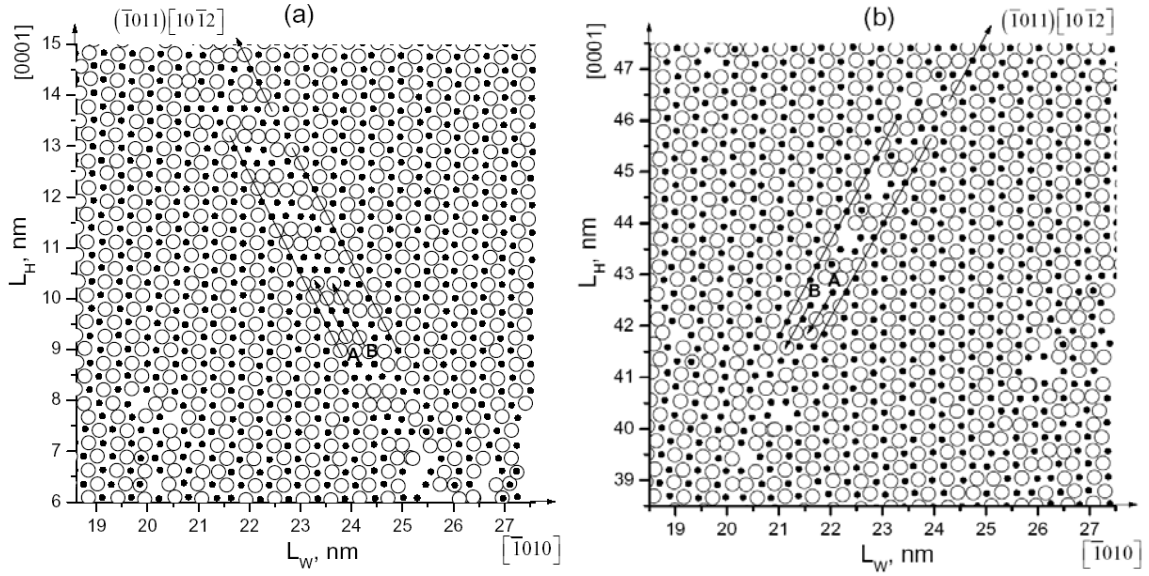

Fig.5. Atomistic structure of shear bands: (a) at 250 K; and (b) at 350 K. Open and solid circles indicate atoms in A and B layers.

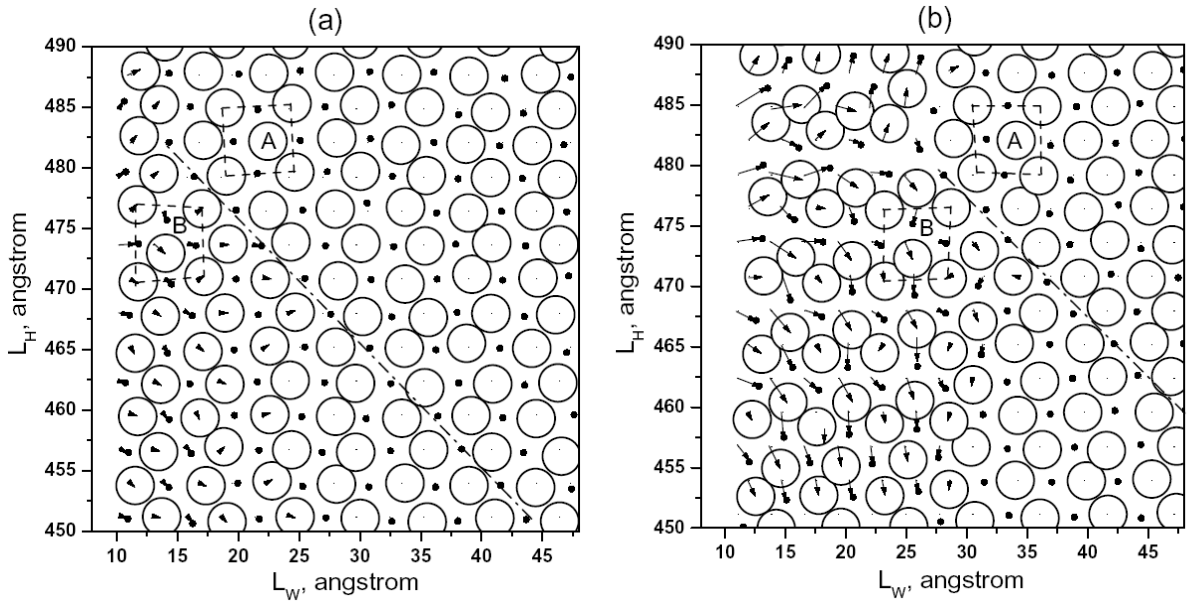

Fig. 6. The formation of a $\{10\bar{1}2\}$ twin under a c-axis tension at 298 K after: (a) 250 steps relaxation; and (b) 450 steps relaxation. Open and solid circles indicate atoms in A and B layers; $(\bar{1}012)$ planes are marked with dash dot lines; arrows indicate the displacements of atoms.

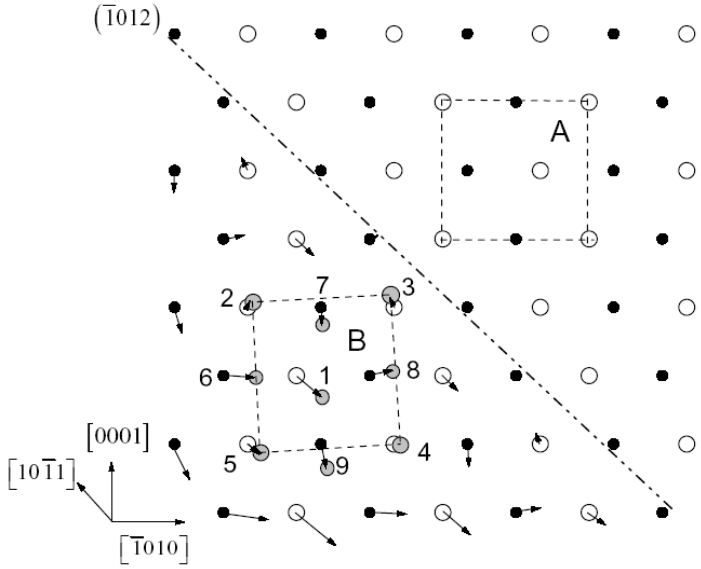

Fig.7. Mechanism of $\{10\bar{1}2\}$ twinning. Open and solid circles indicate atoms in A and B layers; light grey atoms indicate atoms in a twined unit; twin plane is marked with a dash dot line; arrows indicate the displacements of atoms.

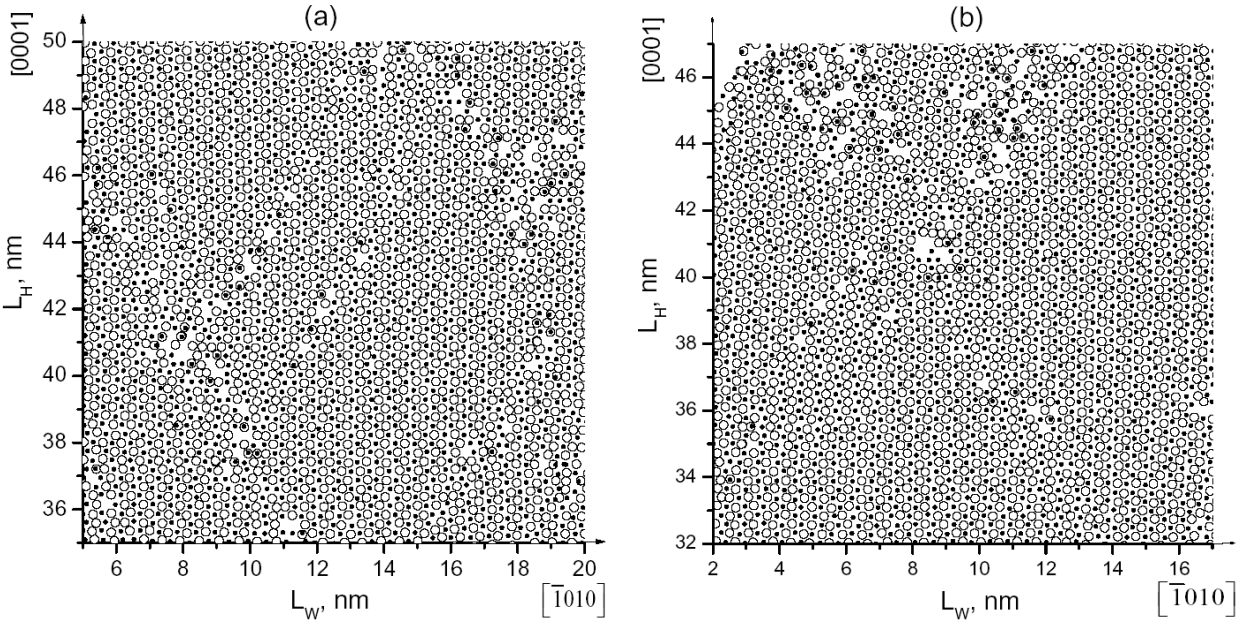

Fig.8. Atomistic structure of slip traces at: (a) 500 K; and (b) 570 K. Open and solid circles indicate atoms in A and B layers.